JOURNAL OF MATERIALS SCIENCE 31 (1996) 6077–6083

High temperature creep behaviour of single crystal oxides

SHIQIANG DENG*
Central Iron and Steel Research Institute, 100081 Beijing, Peoples Republic of China

The creep resistance of several single crystal oxides is evaluated on the basis of creep data from different sources using a Larson–Miller (L–M) method. The possible creep mechanisms involved in high temperature creep deformation of single crystal oxides are discussed by comparing the collected creep data with theoretical creep models. The high temperature creep of single crystal oxides is generally considered as a diffusion-controlled process: dislocation climb controlled by the lattice diffusion of the slowest moving species (power law) at moderately high stresses, Harper–Dorn creep at low stresses, and power law breakdown at high stresses. The relative comparison of the creep data from different sources using the L–M method and the general analysis about the high temperature creep behaviour indicate that single crystal oxides with a precise stoichiometric composition, complex crystal structure and selected orientation such as [111] oriented YAG ($Y_3Al_5O_{12}$), *c*-axis Al_2O_3, [110] oriented $MgAl_2O_4$ are potential candidates as reinforcements for very high temperature structural applications.

1. Introduction

Continuous ceramic fibre-reinforced ceramic matrix composites (CMC's) are considered to be more promising candidates for structural applications than monolithic ceramics because of their increased fracture toughness and reliability. The performance of continuous ceramic fibre-reinforced CMC's at high temperature strongly depends on the thermo-mechanical stability of the reinforcing ceramic fibres. In turn, the high temperature thermo-mechanical stability of the fibres is determined mainly by their resistance to oxidation and creep. Non-oxide fibres such as carbon fibres and silicon carbide fibres potentially exhibit good creep resistance, but they are very sensitive to oxidation in a high temperature oxidizing environment. From a chemical view point, oxide fibres should provide the greatest stability in an oxidizing atmosphere, unfortunately however the inadequate creep resistance of the currently available oxide fibres impairs their application as reinforcements in CMC's intended for very high temperature service [1].

Investigations have shown that a few single crystal oxides may be capable of providing good high temperature creep resistance and strength [2–17], presumably because they lack the grain boundaries that are a source of creep deformation for polycrystalline materials. Hence, in the search for candidate reinforcements intended for very high temperature service the creep behaviour of single crystal oxides has attracted attention.

So far, several isolated investigations have been undertaken on the creep properties of single crystal oxides. In order to make a meaningful comparison of the creep data from different sources a Larson–Miller (L–M) treatment has been used in our previous paper [18], which enabled a direct comparison of the creep resistance of different single crystal oxides. In this paper a further evaluation is made of the relative creep resistance of several single crystal oxides by compiling their L–M plots together using the same constant, *C*. A discussion regarding their potential high temperature creep mechanisms is presented by comparing the creep data from different sources with possible creep mechanisms.

The main objectives of this work are to make best use of the available creep data from different creep tests and to find ways of identifying the greater creep resistant materials based on considerations of high temperature creep mechanisms, compositions and crystal structures.

2. The relative creep resistance of some single crystal oxides

The L–M treatment as proposed by Larson and Miller for obtaining a time–temperature relationship for rupture and creep stresses [19] provides a simple method to evaluate the creep resistance of a material with limited creep data. The basis of the L–M method is that the creep process can be considered to be

* Present address: Centre for Advanced Materials Technology, Department of Mechanical Engineering, University of Sydney, 2006 NSW, Australia

0022–2461

thermally activated and consequently for a given applied stress the creep rate is described by an Arrhenius-type expression of the form:

$$\dot{\varepsilon} = A\exp(-Q/RT) \quad (1)$$

where $\dot{\varepsilon}$ is the steady state creep rate, Q is the activation energy for the creep process, T is the absolute temperature in Kelvin, R is the gas constant and A is a constant. Equation 1 can also be written as

$$Q/R = T(\ln A - \ln \dot{\varepsilon}) \quad (2)$$

Introducing the concept of a creep life, t_s, defined as the time taken for the steady state creep rate to yield a given arbitrary strain, ε_x (it can be fixed at a certain value):

$$t_s = \varepsilon_x/\dot{\varepsilon} = constant/\dot{\varepsilon} \quad (3)$$

Equation 2 can then be written as:

$$L = Q/R = T(C + \log t_s) \quad (4)$$

where L is the so-called L–M parameter and C is a constant, which can be extracted from a plot of log t_s versus $1/T$ on the basis of a rearrangement of Equation 4. Assuming Q to be independent of temperature, the value of L at a given stress for a given material is considered to be constant, which implies that there is a fixed relationship between T and t_s. Moreover it is generally found that L is inversely proportional to the logarithm of applied stress ($\log\sigma$) to yield a single straight line. Creep data appropriate to other combinations of stress–temperature lifetime can then be predicted from the L–M plot by interpolation or extrapolation. The derived relationship between σ, t_s and T is relatively insensitive to the value of the constant C as shown in our previous paper [18], and it is often set at a fixed value when considering a group of related materials.

Fig. 1 shows the L–M plot using the compressive creep data from different sources. The creep data were obtained by constant load or constant stress compression except for the Al_2O_3–$Y_3Al_5O_{12}$ (Al_2O_3-YAG) eutectic which was crept by constant strain rate. A value of 20 for the constant C was chosen to calculate the L–M parameters because most of the derived values for C are around 20 [18] and where more than one value of the L–M parameter existed for a given applied stress an average value was used in the plot. The variable, t_s, is an inverse measure of the steady state creep rate ($t_s = \varepsilon_x/\dot{\varepsilon}_s$). ε_x was chosen as 10^{-5} in the present work, which is based on the general creep strain limitation for materials in high temperature application [20].

Fig. 2 is the L–M plot of some single crystal oxides using the data from tensile creep tests. A value of 10 was used for the constant C based on the derived values for these oxides in tensile creep tests [18].

Inspection of Figs 1 and 2 shows that c-axis Al_2O_3, YAG with a [1 1 1] orientation and $MgAl_2O_4$ spinel with a [1 1 0] orientation exhibit the best creep resistance. It is also seen that the creep resistance of some single crystal oxides is very anisotropic. For example in the case of single crystal Al_2O_3, a small deviation of the crystal orientation from the c-axis can cause a sharp decrease of creep resistance.

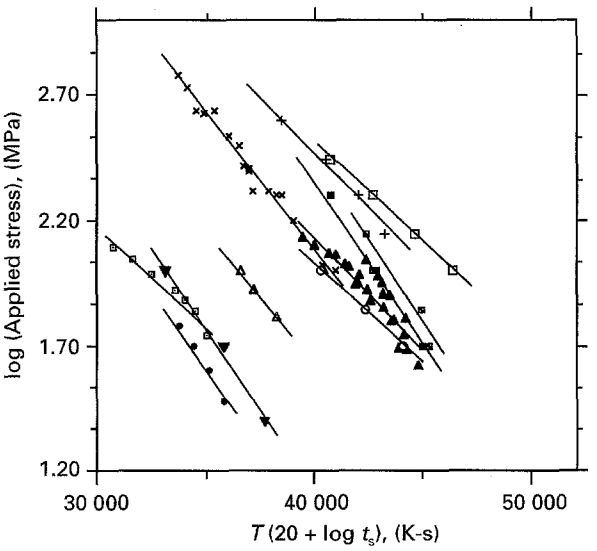

Figure 1 The L–M plot of compressure creep data for; (●) V doped [110] Mg_2SiO_4 [2], (■) [111] $MgO \cdot 0.9Al_2O_3$ [3], (+) [0001] Al_2O_3 [4], (▼) 42° to [0001] Al_2O_3 [4], (×) Al_2O_3-YAG eutectic [5], (□) [111] YAG [4], (△) [$\bar{1}\bar{1}$2] YSZ [6], (○) [110] ThO_2 [4], (⊡) ⟨100⟩ UO_2 [7], (⊠) [1$\bar{1}$00] BeO [4] and (▲) ⟨110⟩ Y_2O_3 [8].

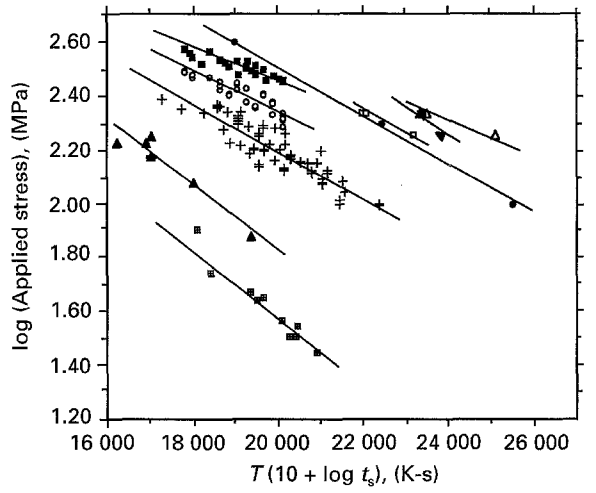

Figure 2 The L–M plot of tensile creep data for; (△) c-axis Al_2O_3 fibre [9], (□) commercial c-axis Al_2O_3 [9], (●) Al_2O_3 fibre (< 2° to c-axis) [10], (▲) Al_2O_3 fibre (24° to c axis) [11], (■) c axis Al_2O_3 filament [12], (○) Ti^{4+} doped c axis Al_2O_3 [13], (+) a axis Al_2O_3 filament [14], (⊞) ⟨011⟩ MgO slab [15] and (▼) [110] spinel fibre [16].

3. General feature about the high temperature creep of single crystal oxides

The creep of ceramics has been reviewed by Cannon and Langdon [21, 22]. The creep mechanisms of ceramics were divided into two groups: lattice mechanisms and boundary mechanisms. Lattice mechanisms are based on the intragranular motion of dislocations. Many theoretical mechanisms have been developed for the intragranular motion of dislocations and are

summarized in Table I of reference [21]. For high temperature creep ($T > 0.5T_m$), a detailed description of the principles underlying the relevant mechanisms has been given by Weertman [23].

For single crystal oxides, lattice mechanisms should be the rate-controlling processes because there are no grain boundaries and thus boundary mechanisms can be neglected. Nevertheless, subgrain creep may be involved. Several mechanisms may be attributed to the high temperature creep process. However, the most likely mechanisms involved in the creep process of single crystal oxides are Harper–Dorn creep, power law breakdown and subgrain creep [21].

In the high temperature regime, dislocations can climb as well as glide. If a gliding dislocation is held up by an obstacle, for example, an obstacle created by other dislocations (fluctuating internal stress field or localized tangles or barriers formed by mutually locked-up dislocations), a little climb may release it, allowing it to glide to the next set of obstacles where the process is repeated. The obstacles can also dissolve away by climb-controlled mutual annihilation of the dislocations as described by the Weertman model [23, 24]. Dislocation climb itself is controlled by diffusion, which is thermally activated. Therefore the important feature of the mechanisms which are based on this climb-plus-glide sequence [23] in the creep process of single crystal oxides should be that the rate-controlling process, at an atomic level, is the diffusive motion of single ions or vacancies to or from the climbing dislocation, rather than the activated glide of the dislocation itself.

At temperature above $0.5T_m$ the steady state creep rate, $\dot{\varepsilon}$, for the creep deformation controlled by dislocation climb can be described by the Nabarro creep equation [25]:

$$\dot{\varepsilon} = \alpha(\pi D_l \beta^2/b^2)(\sigma/G)^3(G\Omega/kT) \quad (5)$$

where α is a constant (estimated by Nabarro to have the value $\alpha \approx 0.01$ and by Weertman to be $\alpha \approx 0.1$) [23]. Ω is the atomic volume ($\sim 0.7b^3$), β is the constant ($\beta \approx 1$) that appears in the equation for the dislocation density, $\rho = (\beta\sigma/Gb)^2$, D_l is the diffusion coefficient for lattice self-diffusion, σ is the applied stress, G is the shear modulus, b is the Burgers vector, k is Boltzmann's constant, and T is the absolute temperature. In the Nabarro creep equation the steady state creep rate is determined by the dislocation density ($\rho \propto \sigma^2/G^2b^2$) and the velocity of dislocation climb ($v \propto \Omega D_l\sigma/kT$). Equation 5 can be simplified to ($\alpha \approx 0.01$ was used);

$$\dot{\varepsilon} = 0.022\frac{D_l Gb}{kT}\left(\frac{\sigma}{G}\right)^3 \quad (6)$$

At sufficiently low stresses, Harper–Dorn creep [26] may occur, which gives the simple relationship:

$$\dot{\varepsilon} = A_{HD}\frac{D_l Gb}{kT}\left(\frac{\sigma}{G}\right) \quad (7)$$

where A_{HD} is a dimensionless constant. The most plausible explanation for this process is that Harper–Dorn creep occurs when climb-controlled creep is under conditions such that the dislocation density does not change with stress. Thus the creep rate, $\dot{\varepsilon}$, is proportional to the applied stress. It was considered that Harper–Dorn creep arises from the climb of edge dislocations under saturated conditions at a very low applied stress [27, 28].

At high stresses, a breakdown of power law creep may appear. The creep process is transformed from diffusion-controlled dislocation climb to glide controlled flow (or both) and the creep rate in this process is greater than that in the power law process [23].

For single crystals with a high dislocation density, subgrain boundaries may form and they will have an influence on the creep process. Several subgrain creep mechanisms have been proposed and reviewed by Weertman [23]. Since the dislocations making up the subgrain boundary undergo climb motion, this type of creep is also a dislocation climb-controlled process.

At low values of the applied stress (about 10^{-5}–$10^{-4}\,G$) a stress exponent of unity has been found for CaO, UO_2 and MgO single crystals [29–33]. Harper–Dorn creep was considered as the dominant deformation mechanism for this stress regime. When moderately high values of the stresses were applied, a transition from Harper–Dorn creep to power law creep with a stress exponent of $\sim$ 3–5 has also been found for these single crystal oxides [29–33].

The creep data from different sources were plotted with normalized creep rate against normalized stress and compared with the possible creep mechanism as described by Equation 6 in order to identify the possible creep mechanisms of some other single crystal oxides. Fig. 3 schematically summarizes the creep data for single crystal Al_2O_3 with various orientations shown in the figure. The creep data are from tensile creep tests except the data indicated [4, 9–11, 17, 34]. The dashed line in Fig. 3 shows the prediction of Equation 6 for a dislocation climb mechanism in a power law regime with a stress exponent $n = 3$. The values of the material parameters used for the figure are shown in Table I. The diffusion coefficient, D_l, was

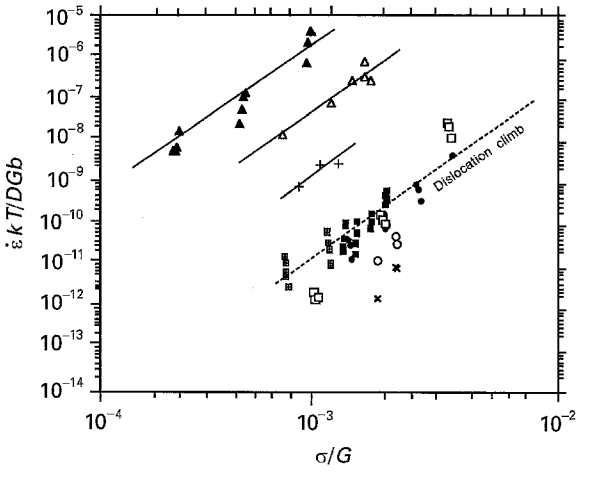

Figure 3 Normalized creep rate plotted against normalized stress for single crystal Al_2O_3. Data plotted for; (×) c axis fibre [9], (□) 0–2° to c axis [10], (■) 0–2.5° to c axis [17], (+) 6° to c axis [17], (⊞) 0° to [0001] [34], (△) 24° to c axis fibre [11], (○) commercial c axis fibre [9], (●) Al_2O_3 [0001] [4] and (▲) 42° to [0001] (in compression) [4].

TABLE 1 Material parameter values [35]

	Al_2O_3	$MgAl_2O_4$
Burger's vector, b (m)	4.76×10^{-10}	5.71×10^{-10}
Melting temperature $T_m(K)$	2320	2408
Shear modulus at 300 K, G_0 (MPa)	1.55×10^5	9.92×10^4
Temperature dependence of modulus, $T_m/G_0\ dG/dT$ [a]	-0.35	-0.22
Lattice diffusion coefficient, $D_l(O^{2-})(m^2s^{-1})$	$0.19\exp(-636000/RT)$	$8.9 \times 10^{-5}\exp(-439000/RT)$

[a] $G = G_0\left[1 + \frac{T-300}{T_m}\left(\frac{T_m\,dG}{G_0\,dT}\right)\right]$

taken as the O^{2-} lattice diffusion coefficient because it is the slowest moving species in this system [35].

For Al_2O_3 single crystals with orientations close to the c-axis, the creep datum points are close to the prediction of dislocation climb creep, but for the crystals with orientations 6–42° from the c-axis, the datum points are well above the prediction line. However, the stress exponents for all crystals are about ~ 3–4, which means that the datum points are all within the power law regime and indicates that dislocation climb controlled power law creep is the dominant mechanism for these single crystals under applied stress $\sigma \approx 2 \times 10^{-4} - 3 \times 10^{-3}G$.

The plastic deformation of sapphire (α-Al_2O_3) has been extensively studied in recent decades. It is considered that at low temperatures prismatic plane slip occurs and at elevated temperatures basal slip is the easiest slip system and pyramidal slip the hardest to activate [36, 37]. In high temperature creep tests when stress is applied parallel to the c-axis of a Al_2O_3 single crystal, basal and prismatic slip in the crystal are suppressed. In order to activate pyramidal slip a higher stress must be applied and, as a result, c-axis sapphire single crystal can exhibit excellent creep resistance. The work of Unal *et al.* [10] on the creep of c-axis oriented sapphire fibre proved that over the temperature range of 1400–1800 °C and stress range of 100–400 MPa pyramidal slip occurs. The crept sample was faceted and had slip features on the surface. Analysis revealed that primary dislocations with $1/3\langle 1\bar{1}01\rangle$ Burgers vectors glided on $\{1\bar{1}02\}$ and $\{11\bar{2}3\}$ pyramidal planes and secondary dislocations having $1/3\langle 11\bar{2}0\rangle$ Burgers vectors formed on the basal plane as a result of dislocation reactions on the pyramidal planes. Activation parameters and microstructural observations indicated that dislocation climb controlled the overall deformation process.

The higher creep rates for some crystals oriented with a deviation from the c-axis as shown in Fig. 3 may be due to possible basal plane slip caused by the resolved shear stress. As analysed by Firestone and Heuer [34] a small misorientation can make the resolved shear stress on the basal plane high enough to activate the basal slip and increase creep rate. Nevertheless, the creep process is still controlled by dislocation climb because dislocation cross-slip is very difficult in single crystal sapphire, which is determined by the nature of its crystal structure and defects.

Fig. 4 shows the normalized creep rate versus normalized stress for Y_2O_3 stabilized ZrO_2 single crystals using compressive creep data [4, 6, 38] and the material parameters listed in Table II. From Fig. 4 it can be seen that the creep datum points are in a power law regime when stresses are less than $10^{-3}G$, but when the stress exceeds about $10^{-3}G$, the power law appears to break down since there is an obvious transition in the stress exponent (stress exponent $n > 6$).

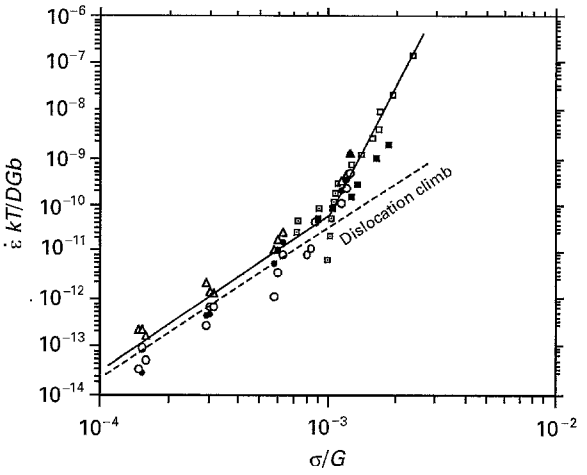

Figure 4 Normalized creep rate versus normalized stress for Y_2O_3 stabilized ZrO_2 single crystals. Data are presented for; (■) $\langle 112\rangle$ in argon [38], (□) $\langle 112\rangle$ in air [38], (⊡) $[\bar{1}\bar{1}2]$ [6], (△) [111] [4], (●) [110] [4] and (○) [100] [4].

Fig. 5 is the normalized creep rate versus normalized stress plot for several $MgO.nAl_2O_3$ single crystals on the basis of the creep data of both compressive and tensile tests [3, 16, 39–42] and material parameters listed in Table I. A power law creep can be observed in this plot and higher creep rates appear with increasing non-stoichiometry for Al_2O_3 rich crystals, which indicates that high temperature creep of Al_2O_3 rich spinels depends strongly on the composition ratio n = Al_2O_3/MgO. However, MgO rich spinels exhibit a creep resistance which is comparable with that of stoichiometric spinel and is better than that of Al_2O_3 rich spinels.

4. Discussion

As described above, the high temperature creep of single crystal oxides at low stresses (Harper–Dorn creep) and at moderately high stresses (power law creep) consists mainly of a dislocation climb process controlled by the diffusion of the slowest moving species, and even at high stresses (power law breakdown) the creep deformation may also be greatly affected by the diffusion process of the slowest moving species.

TABLE II Material parameters for ZrO_2 [21][a]

Lattice diffusion coeffient, $D_l(Zr^{4+})$, $(m^2 s^{-1})$[b]	Shear modulus, G_0(MPa)	ΔG ($MPaK^{-1}$)	Burgers vector, b (m)
$3.5 \times 10^{-6} \exp(-387000/RT)$	1.54×10^{-5}	35.2	2.57×10^{-10}

[a] $G = G_0 - (\Delta G)T$

[b] Lattice diffusion coefficient, $D_l(Zr^{4+})$, is used becuase the diffusion of Zr^{4+} in ZrO_2 is slower than that of O^{2-}.

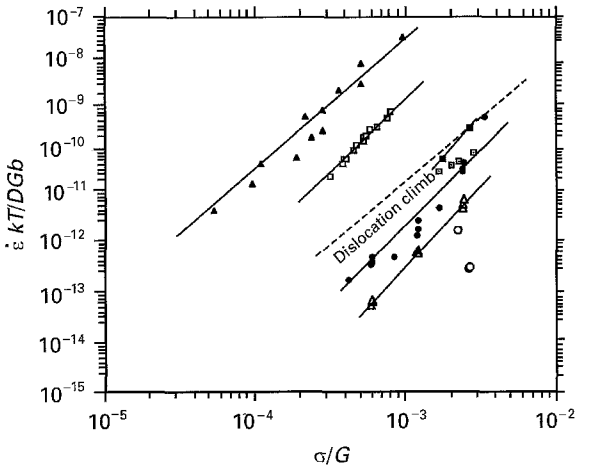

Figure 5 Normalized creep rate versus normalized stress for $MgO \cdot nAl_2O_3$ single crystals. Data are presented for; (▲) $MgO \cdot 3.0\ Al_2O_3$ ⟨100⟩ [42], (□) $MgO \cdot 1.8Al_2O_3$ ⟨100⟩ [40], (■) $MgO \cdot 1.1Al_2O_3$ ⟨100⟩ [41], (○) $MgO \cdot Al_2O_3$ [110] fibre [16], (⊡) $MgO \cdot Al_2O_3$ 45° from (111) and (101) [39], (●) $MgO \cdot 0.9\ Al_2O_3$ [100] [3] and (△) $MgO \cdot 0.9Al_2O_3$ [111] [3].

Therefore, variables that influence the diffusion process must also affect the creep behaviour of a material. In addition to external factors such as temperature and stress, some material parameters will influence the high temperature creep of single crystal oxides via effects on the diffusion of ions and vacancies. Moreover, the characteristics of defects such as vacancies and dislocations in the oxides also determine their high temperature creep behaviour.

4.1. Crystal structure

The specific properties of a ceramic in a crystal structure are determined by their having sublattices partially or totally occupied by ions of various natures, sizes and electrical charges. The crystal structure is the result of a compromise between steric and electrostatic requirements; it determines the nature of point defects, the structure of dislocations, as well as the possible interaction between these defects.

Simple oxides generally consist of two opposite electrically-charged ions. For some symmetric simple oxides such as CaO and MgO (NaCl structure) in which oxygen ions occupy the fcc positions while metal ions occupy the interstices, when a dislocation moves from one site to the nearest adjacent site on the oxygen plane no change occurs in the local ionic environment and thus oxides with an NaCl-type structure do not exhibit good creep resistance. Oxides with hexagonal close-pack (hcp) structure such as α-Al_2O_3 and BeO are the other class of close-packed oxide materials. In α-Al_2O_3 oxygen ions are packed in a close-packed hexagonal arrangement, aluminium ions reside in the octahedral interstitial sites and each aluminium ion is surrounded by six equidistant oxygen ions. In this arrangement only two-thirds of the octahedral interstitial sites are occupied by cations and there are some ordered vacant sites within each close-packed oxygen layer. To compromise the balance of charges and sites some oxygen anions must undulate their sites slightly, and, as a result, the cores of the oxygen anions deviate from their ideal positions. Therefore, dislocation slip on these oxygen planes must require overcoming a greater barrier than if the planes were ideal. That is why α-Al_2O_3 single crystals generally exhibit a good creep resistance. For some complex oxides, such as YAG (even though it is cubic) and spinel (complex cubic), the oxygen packing becomes distorted and can vary from position to position within the unit cell. Such complex structures must severely inhibit dislocation slip and the creep deformation at high temperature can reasonably be considered as a process controlled by a the climb-plus-glide sequence as described above.

4.2. Crystallographic anisotropy

Single crystals are anisotropic in crystal structure. The Peierls forces for dislocation glide between different crystal planes are different; dislocations glide more easily on close-packed planes (with large distance between planes) because their cores are more widely spread in them, which leads to a lower Peierls stress (or lower lattice friction). Moreover, since diffusion is the motion of ions or vacancies in the crystal lattice, differences in the arrangement of species in the lattice along different crystallographic directions must influence the diffusion rates of species in these directions. As a result, the creep resistance of most single crystal oxides strongly depends on the stress axis orientation. As shown in Figs 1 and 2, an oxide such as single crystal Al_2O_3 exhibits different creep rates with different orientations.

4.3. Crystal defects

Point, line and surface imperfections in a single crystal, depending on whether the defects are vacant sites or interstitial atoms, various types of dislocations, and also stacking faults should have influence on diffusion and thus the creep of the material. The characteristics of point defects and dislocations in oxides have been reviewed by Mitchell *et al.* [43, 44]. The point defects

that are generally found in oxides include oxygen vacancies, cation vacancies, oxygen interstitials and cation interstitials. The variation of crystal composition can cause non-stoichiometry in oxides such as in the case of Al_2O_3 rich $MgO \cdot nAl_2O_3$ in which there is an increase in cation vacancies with increasing the ratio, n ($n > 1$) and, as a result, the creep resistance is decreased because the dislocation climb process is accelerated by the increased vacancy concentration as is shown in Fig. 5. The dislocation dissociations which have been observed in oxides preserve the integrity of the anion sublattice, giving a fault of the cation lattice. For the oxides which have been analysed in most detail such as Al_2O_3 and $MgO \cdot nAl_2O_3$, dislocation dissociation occurs in most cases by the separation of partial dislocations via a climb rather than a glide process. It was shown that the climb dissociated configuration has a slightly lower energy than the glide configuration and that the latter is metastable with respect to the former [44]. These points can be used to explain why diffusion-controlled dislocation climb rather than dislocation gliding is the dominant rate-controlling mechanism. Dislocation climb is a complicated process in oxides and the motion by one unit cell vector of a jog in an edge dislocation involves the transport of several oxygen anions and cations. Therefore those factors which determine the diffusion rates of ions and vacancies in single crystal oxides will influence their creep behaviour during high temperature deformation.

Based on the analysis of the creep data from different sources and the high temperature creep characteristics of single crystal oxides, it appears that the factors which contribute to high creep resistance are as follows: (a) strong bonding between the cations and anions which is determined by the compromise between steric and electrostatic requirements; (b) a close-packed, irregular and complicated crystal structure which makes dislocation slip and climb difficult; (c) an orientation which suppresses the easier slip systems; (d) a precise stoichiometry which makes a perfect arrangement of cations and anions with low defect concentration; and (e) relatively high melting temperature which determines the strong bonding of cations and anions at high temperature. Single crystal oxides such as YAG, *c*-axis Al_2O_3 and [110] oriented $MgAl_2O_4$ have these qualities, and can be considered as promising candidates for developing reinforcements for CMC's.

5. Summary and conclusions

(1) The Larson–Miller method is an effective approach to evaluate the high temperature creep properties of single crystal oxides.

(2) The high temperature creep of single crystal oxides generally occurs via a diffusion-controlled process. These include dislocation climb controlled by the lattice diffusion of the slowest moving species at moderately high stresses (power law creep), Harper–Dorn creep at low stresses, and power law breakdown at high stresses. The factors that hinder dislocation motion, especially dislocation climb, and decrease the lattice diffusion rate of the slowest moving species in an oxide increase its creep resistance.

(3) The results of a comparison of creep data from different sources using the L–M method and a general analysis of high temperature creep behaviour indicates that single crystal oxides with a precise stoichiometric composition, complex crystal structure and selected orientation such as YAG, *c*-axis Al_2O_3 and [110] oriented $MgAl_2O_4$ are promising candidates as reinforcements in CMC's intended for high temperature structural applications.

Acknowledgements

This work was undertaken while the author was in the Department of Materials Science and Production Technology, Lulea University, Sweden, as a visiting researcher. The author would like to thank Professor Richard Warren for his guidance and Dr W. B. Li for his helpful discussions about creep mechanisms.

References

1. J. A. DICARLO, *Composites Sci. Technol.* **51** (1994) 213.
2. D. L. RICOULT and D. L. KOHLSTEDT, *J. Amer. Ceram. Soc.* **69** (1986) 770.
3. G. S. CORMAN, *J. Mater. Sci. Lett* **11** (1992) 1657.
4. *Idem, Ceram. Engng Sci. Proc.* **12** (1991) 1745.
5. T. A. PARTHASARATHY and TAI-IL MAH, *J. Amer Ceram. Soc.* **76** (1993) 29.
6. J. MARTINEZ-FERNANDEZ, M. JIMENEZ-MELENDO, and A. DOMINGUEZ-RODRIGUEZ, *ibid* **73** (1990) 2452.
7. M. S. SELTZER, A. H. CLAUER and B. A. WILCOX, *J. Nucl. Mater.* **44** (1972) 43.
8. P. R GABORIAUD, *Phil. Mag. A* **44** (1981) 561.
9. J. S. HAGGERTY and K. C. WILLS, *Ceram. Engng. Sci. Proc.* **12** (1991) 1785.
10. O. UNAL, K. P. D. LARGERLOF, and G. S. CORMAN, *Ceram. Engng Sci. Proc.* **14** (1993) 600.
11. J. R. PORTER, *Mater. Sci. Engng* **A166** (1993) 179.
12. R. E. TRESSLER and D. J. BARBER, *J. Amer. Ceram. Soc.* **57** (1974) 13.
13. D. J. MICHAEL and R. E. TRESSLER, *J. Mater. Sci.* **9** (1974) 1781.
14. D. M. KOTCHICK and R. E. TRESSLER, *J. Amer. Ceram. Soc.* **63** (1980) 429.
15. A. H. CLAUER and B. A. WILCOX, *ibid* **59** (1976) 89.
16. J. SIGALOVSKY, K. C. WILLS and J. S. HAGGERTY, *Ceram. Engng Sci. Proc.* **13** (1992) 183.
17. D. J. GOOCH and G. W. GROVES, *J. Mater. Sci.* **8** (1973) 1238.
18. S. DENG and R. WARREN, *J. Euro. Ceram. Soc.* **15** (1995) 513.
19. F. R. LARSON and J. MILLER, *Trans. ASTM* **74** (1952) 765.
20. I. E. COURTRIGHT, *Ceram. Eng. Sci. Proc.* **12** (1991) 1725.
21. W. R. CANNON and G. LANGDON, *J. Mater. Sci.* **18** (1983) 1.
22. *Idem, ibid* **23** (1988) 1.
23. J. WEERTMAN in "Rate Processes in Plastic Deformation of Materials", edited by J. C. M. Li and A. K. Mukherjee, (American Society for Metals, Metals Park, Ohio, 1975) p. 315.
24. *Idem, Trans. ASM* **61** (1968) 681.
25. F. R. N. NABARRO, *Phil. Mag.* **16** (1967) 231.
26. J. HARPER and J. E. DORN, *Acta Metall* **5** (1957) 654.
27. F. A. MOHAMED, K. L. MURTY and J. W. MORRIS in "Rate Processes in Plastic Deformation of Materials", edited by J. C. M. Li and A. K. Mukherjee, (American Society for Metals, Metals Park, Ohio, 1975) p. 459.
28. T. G. LANGDEN and P. YAVARI, *Acta Metall* **30** (1982) 881.

29. P. J. DIXON-STUBBS and B. WILSHIRE, *Phil. Mag. Ar* **45** (1982) 519.
30. T. G. LANGDON, *ibid* **47** (1983) L29.
31. O. A. RUANO, J. WOLFENSTINE, J. WADSWORTH and O. D. SHERBY, *Acta Metall.* **39** (1991) 661.
32. K. S. RAMESH, E. YASUDA and S. KIMURA, *J. Mater. Sci.* **21** (1986) 3147.
33. O. A. RUANO, J. WOLFENSTINE, J. WADSWORTH and O. M. SHERBY, *J. Amer. Ceram. Soc.* **75** (1992) 1737.
34. R. F. FIRESTONE and A. H. HEUER, *ibid* **59** (1976) 24.
35. H. J. FROST and M. F. ASHBY, "Deformation-Mechanism Maps", (Pergamon, Oxford, 1982).
36. K. P. D. LARGERLOF in "Deformation of Ceramic Materials II", edited by R. E. Tressler and R. C. Bradt, (Plenum, New York, 1984), p. 199.
37. K. P. D. LARGERLOF and A. H. HEUER, *J. Amer. Ceram. Soc.* **77** (1994) 385.
38. M. JIMENEZ-MELENDO, J. MARTNEZ-FERNANDEZ, A. DOMINGUEZ-RODRIGUEZ and J. CASTING, *J. Eur. Ceram. Soc.* **12** (1993) 97.
39. L. HWANG, A. H. HEUER and T. E. MITCHELL in "Deformation of Ceramic Materials", edited by R. C. Bradt and R. E. Tressler, (Plenum, New York, 1975), p. 257.
40. R. DUCLOS, N. DOUKHAN and B. ESCAIG, *J. Mater. Sci.* **13** (1978) 1740.
41. *Idem, Acta Metall.* **30** (1982) 1381.
42. R. D. MACBRAYER, Ph.D. thesis, North Car. State Univ., Raleigh (USA), (1965).
43. T. E. MITCHELL, L. W. HOBBS, A. H. HEUER, J. CASTAING, J. CADOZ and J. PHILIBERT, *Acta Metall.* **27** (1979) 1677.
44. T. E. MITCHELL, W. T. DONLON, K. P. D. LARGERLOF and A. H. HEUER in "Deformation of Ceramic Materials", edited by R. C. Bradt and R. E. Tressler, (Plenum, New York, 1975), p. 125.

Received 14 June 1995
and accepted 13 June 1996